crystals

MDPI

Supplementary Materials

Modifying HKUST-1 Crystals for Selective Ethane Adsorption Using Ionic Liquids as Synthesis Media

Gregory S. Deyko[1]*, Lev M. Glukhov[1], Vera I. Isaeva[1]*, Vladimir V. Chernyshev[2,3], Vadim V. Vergun[1], Danil A. Arkhipov[1], Gennady I. Kapustin[1], Olga P. Tkachenko[1], Vera D. Nissenbaum[1] and Leonid M. Kustov[1,3]*

[1] N.D. Zelinsky Institute of Organic Chemistry, Russian Academy of Sciences, 47 Leninsky Prospect, 119991 Moscow, Russia; elektron77@mail.ru (L.M.G.); polubrat@mail.ru (V.V.V.); arkhipov.danil2015@gmail.com (D.A.A.); gik@ioc.ac.ru (G.I.K.); ot@ioc.ac.ru (O.P.T.); vdn14@inbox.ru (V.D.N.)
[2] A.N. Frumkin Institute of Physical Chemistry and Electrochemistry, Russian Academy of Sciences, Building 4, 31 Leninsky Prospect, 119071 Moscow, Russia; vladimir@struct.chem.msu.ru
[3] Department of Chemistry, M.V. Lomonosov Moscow State University, 1-3 Leninskie Gory, 119991 Moscow, Russia; vladimir@struct.chem.msu.ru (V.V.C.)
* Correspondence: gdeyko@gmail.com (G.S.D.); veraisaeva2019@mail.ru (V.I.I.), LMK@ioc.ac.ru (L.M.K.)

Citation: Deyko, G.S.; Glukhov, L.M.; Isaeva, V.I.; Chernyshev, V.V.; Vergun, V.V.; Arkhipov, D.A.; Kapustin, G.I.; Tkachenko, O.P.; Nissenbaum, V.D.; Kustov, L.M. Modifying HKUST-1 Crystals for Selective Ethane Adsorption Using Ionic Liquids as Synthesis Media. *Crystals* **2022**, *12*, 279. https://doi.org/10.3390/cryst12020279

Academic Editor: Vladimir P. Fedin

Received: 7 January 2022
Accepted: 16 February 2022
Published: 18 February 2022

I. Synthesis of ionic liquids

1-Butyl-3-methylimidazolium chloride (BMIM Cl)

A mixture of 1-methylimidazole (41 g, 0.5 mol), *n*-butyl chloride (50.9, 0.55 mol) and acetonitrile (200 ml) was placed in a sealed vial and heated with stirring for 48 h at 80 °C. The reaction mixture was concentrated by rotary evaporation and the product was dried in a vacuum for 6 h at 80 °C. The yield was 87 g (99%).

1-Butyl-3-methylimidazolium triflate (BMIM OTf)

A mixture of 1-butyl-3-methylimidazolium chloride (43.67 g, 0.25 mol) and potassium triflate (49.4 g, 0.2625 mol) with 200 ml of acetonitrile was stirred for 24 h at room temperature. The reaction mixture was filtered and concentrated by rotary evaporation.

The crude ionic liquid was dried in a vacuum over 2 h at 80 °C and dissolved in CH_2Cl_2 (400 ml). The obtained solution was extracted with small portions of water (10 ml) until negative reaction with silver nitrate. Dichloromethane was distilled off and the product was dried in a vacuum for 6 h at 80 °C. The yield was 65 g (90%).

NMR ^{1}H, δH (300 MHz, DMSO-d_6): 9.10 (1H, s, Im-2), 7.76 (1H, s, Im-4,5), 7.67(1H, s, Im-4,5), 4.16 (2H, t, N$\underline{CH_2}CH_2CH_2CH_3$), 3.85 (3H, s, N$\underline{CH_3}$), 1.76 (2H, quint, $NCH_2\underline{CH_2}CH_2CH_3$), 1.26 (2H, sext, $NCH_2CH_2\underline{CH_2}CH_3$), 0.88 (3H, t, $NCH_2CH_2CH_2\underline{CH_3}$).

1-Octyl-3-methylimidazolium chloride (OMIM Cl)

A mixture of 1-methylimidazole (41 g, 0.5 mol), *n*-octyl chloride (78.05 g, 0.55 mol) and acetonitrile (200 ml) was placed in a sealed vial and heated with stirring for 48 h at 80°C. The reaction mixture was concentrated by rotary evaporation and the product was dried in a vacuum for 6 h at 80 °C. The yield was 115.3 g (99%).

1-Octyl-3-methylimidazolium chloride (OMIM OTf)

A mixture of 1-octyl-3-methylimidazolium chloride (57.7 g, 0.25 mol) and potassium triflate (49.4 g, 0.2625 mol) with 200 ml of acetonitrile was stirred for 24 h at room temperature. The reaction mixture was filtered and concentrated by rotary evaporation. The crude ionic liquid was dried in a vacuum over 2 h at 80 °C and dissolved in CH_2Cl_2 (400 ml). The obtained solution was extracted with small portions of water (10 ml) until negative reaction with silver nitrate. Dichloromethane was distilled off and the product was dried in a vacuum for 6 h at 80 °C. The yield was 80 g (93%).

NMR ^{1}H, δH (300 MHz, DMSO-d_6): 9.09 (1H, s, Im-2), 7.76 (1H, s, Im-4,5), 7.69 (1H, s, Im-4,5), 4.15 (2H, t, N$\underline{CH_2}CH_2CH_2CH_3$), 3.85 (3H, s, NCH_3), 1.76 (2H, quint, $NCH_2\underline{CH_2}$), 1.25 (10H, m, CH_2), 0.86 (3H, t, $CH_2\underline{CH_3}$).

1-Ethyl-3-methylimidazolium bis(trifluoromethylsulfonyl)imide (EMIM Tf_2N)

1-Ethyl-3-methylidimazolium chloride (14.2 g, 0.1 mol) was dissolved in distilled water (20 ml) and mixed with a solution of lithium bis(trifluoromethylsulfonyl)imide (28.7 g, 0.1 mol) in 20 ml of distilled water and 100 ml of CH_2Cl_2 in a separatory funnel. After shaking the organic layer was separated and washed with small portions of water (10 ml) until negative reaction with silver nitrate. Dichloromethane was distilled off and the product was dried in a vacuum for 6 h at 80°C. The yield was 35 g (89%).

NMR ^{1}H, δH (300 MHz, DMSO-d_6): 8.84 (1H, s, Im-2), 7.28-7.29 (2H, s, Im-4,5), 4.27 (2H, q, N$\underline{CH_2}CH_3$), 3.97 (3H, s, N$\underline{CH_3}$), 1.58 (3H, t, $CH_2\underline{CH_3}$).

II. Heating rates of ILs in the MW field

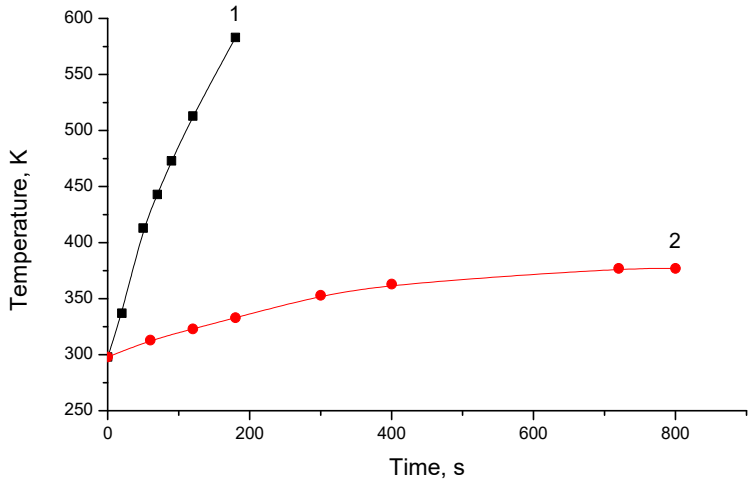

Figure S1. Heating rates of BMIM OTf (1) and water : DMF = 1 : 1 (2) solvent systems in the MW field (2/45 GHz, 200 W).

III. Dependence of the yield of the HKUST-1 material on the reaction time under conditions of the MW-assisted synthesis

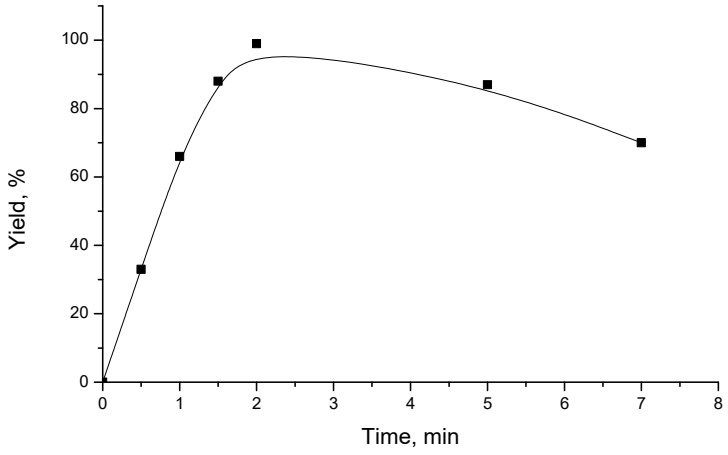

Figure S2. Dependence of the yield of the HKUST-1 material on the reaction time under conditions of the MW-assisted synthesis (2.45 GHz, 200 W). Reaction mixture composition: $Cu(NO_3)_2 \cdot 3H_2O$ (3.63 g, 15 mmol), H_3btc (2.1 g, 10 mmol), EMIM Tf_2N (5 ml).

IV. Elemental analysis data for the synthesized HKUST-1 materials

Table S1. Elemental analysis data for the synthesized HKUST-1 materials.

Material	w(N), %	w(F), %
1solv	<0.1	<0.1
2solv	1.74	1.69
2solv-after-rinsing	<0.1	<0.1
3solv	0.64	traces
3solv-after-rinsing	<0.1	<0.1
8solv	<0.1	<0.1
1mw	<0.1	<0.1
4mw	<0.1	<0.1
5mw	<0.1	<0.1
6mw	<0.1	<0.1
7mw	<0.1	<0.1

V. ^{1}H NMR Spectra of the IL OMIM OTf before and after synthesis

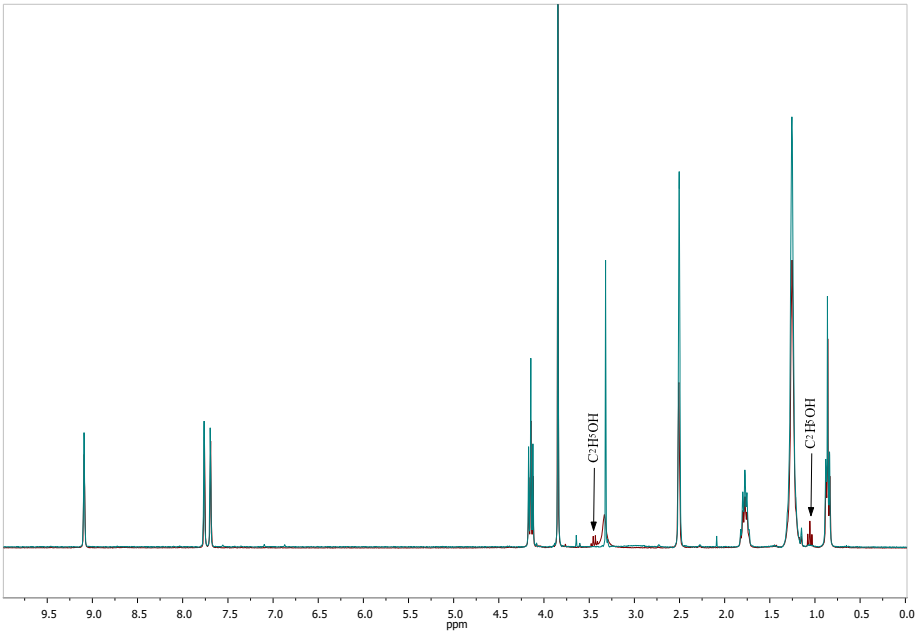

Figure S3. ^{1}H NMR spectra of the neat IL OMIM OTf (green) and of the same IL recycled after synthesis (brown).

VI. XRD studies

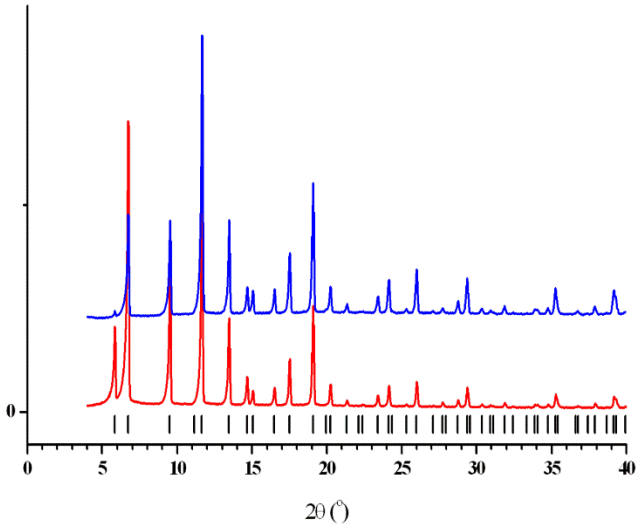

Figure S4. A comparison of experimental XRD patterns of **HKUST-1**$_{\text{DMF-MW}}$ synthesized by MW-technique in DMF as a single solvent (red) and **1mw** (blue) materials. The vertical black bars show the calculated peak positions of the cubic HKUST-1 phase.

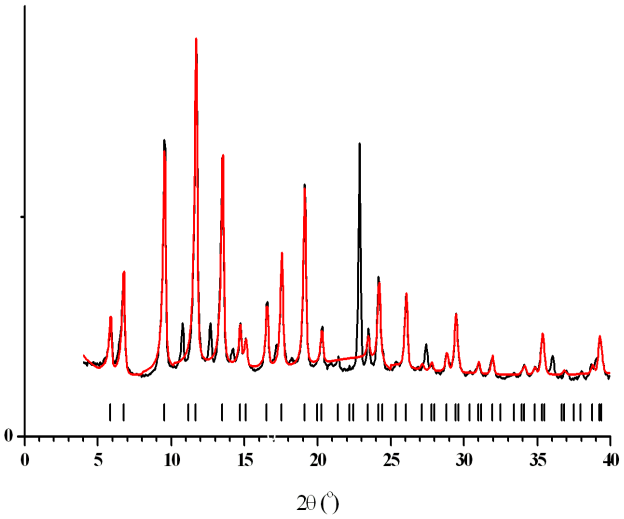

Figure S5. The experimental (black) and calculated by Pawley fitting [1] (red) XRD patterns of the **3solv** sample. The vertical black bars show the calculated peak positions of the cubic HKUST-1 phase.

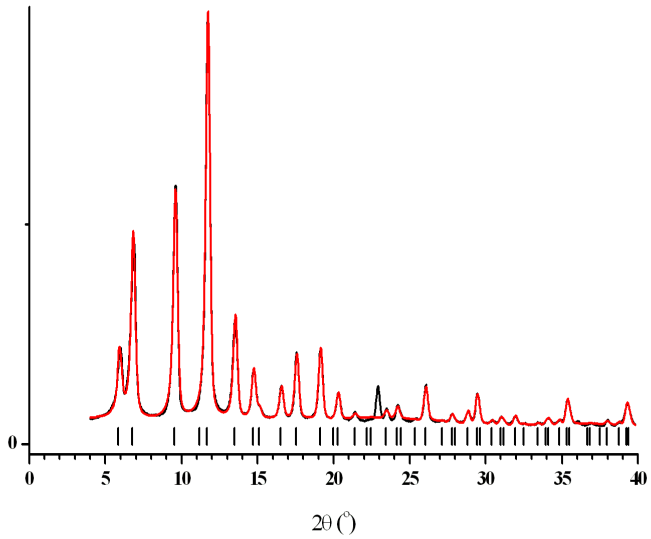

Figure S6. The experimental (black) and calculated by Pawley fitting [1] (red) XRD patterns of the sample **3solv-after-rinsing**. The vertical black bars show the calculated peak positions of the cubic HKUST-1 phase.

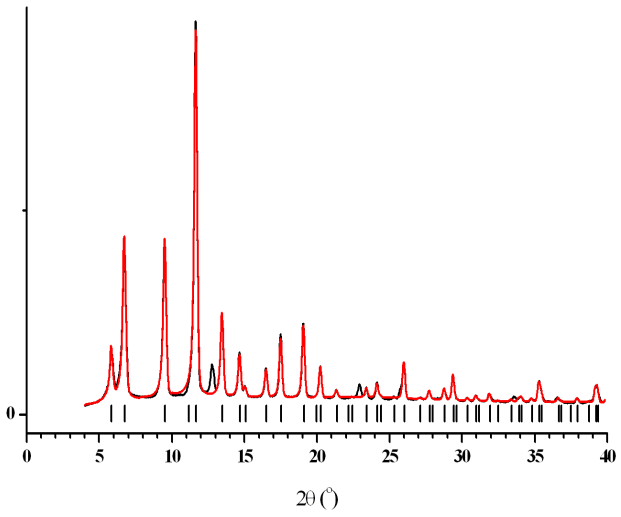

Figure S7. The experimental (black) and calculated by Pawley fitting [1] (red) XRD patterns of the sample **2solv-after-rinsing**. The vertical black bars show the calculated peak positions of the cubic HKUST-1 phase.

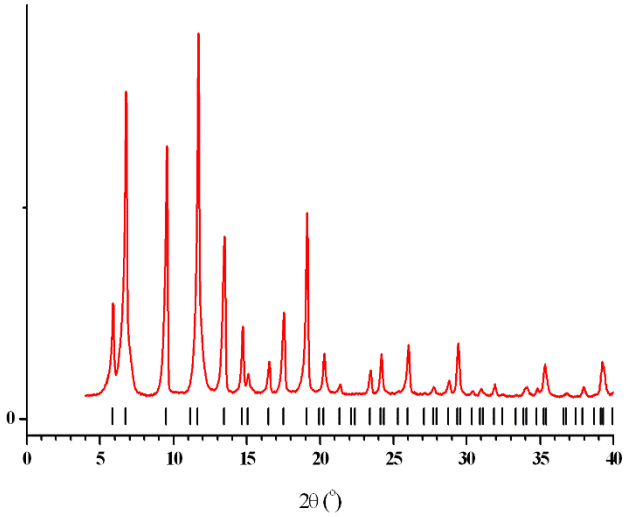

Figure S8. Experimental XRD pattern of HKUST-1 material produced using tenfold quantities of the reagents by MW-technique in DMF-H_2O mixed solvent analogously to the 1mw sample. The vertical black bars show the calculated peak positions of the cubic HKUST-1 phase.

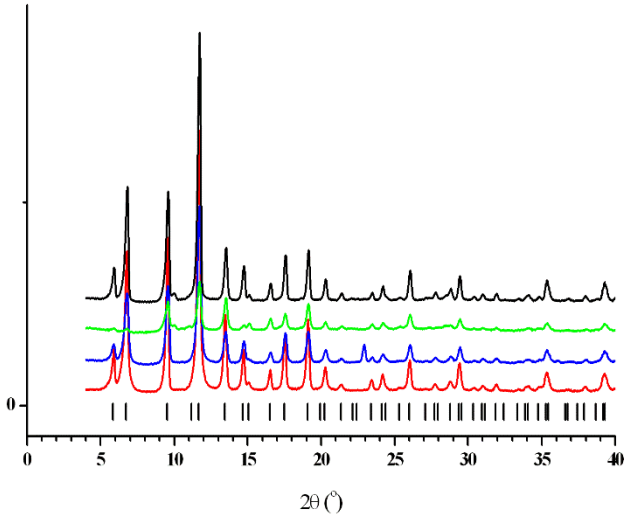

Figure S9. XRD patterns of **1mw** (red), **3solv-after washing** (blue), **8solv** (green), and **5mw** (black) materials soaked in MeOH. The vertical black bars show the calculated peak positions of the cubic HKUST-1 phase.

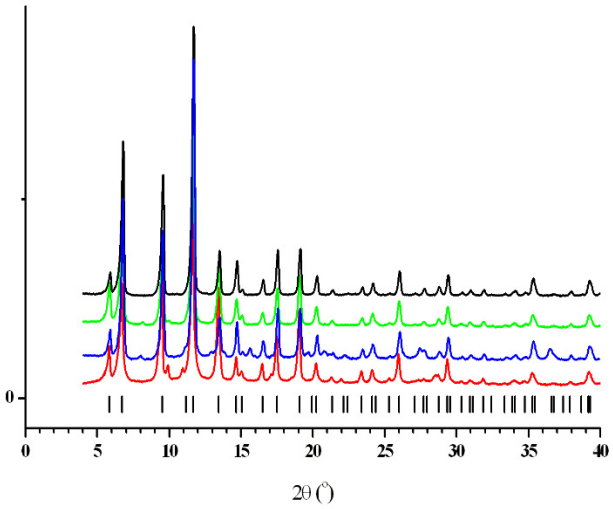

Figure S10. XRD patterns of **1mw** (red), **3solv-after washing (blue)**, **8solv** (green), and **5mw** (black) materials soaked in H_2O. The vertical black bars show the calculated peak positions of the cubic HKUST-1 phase.

VII. SEM images

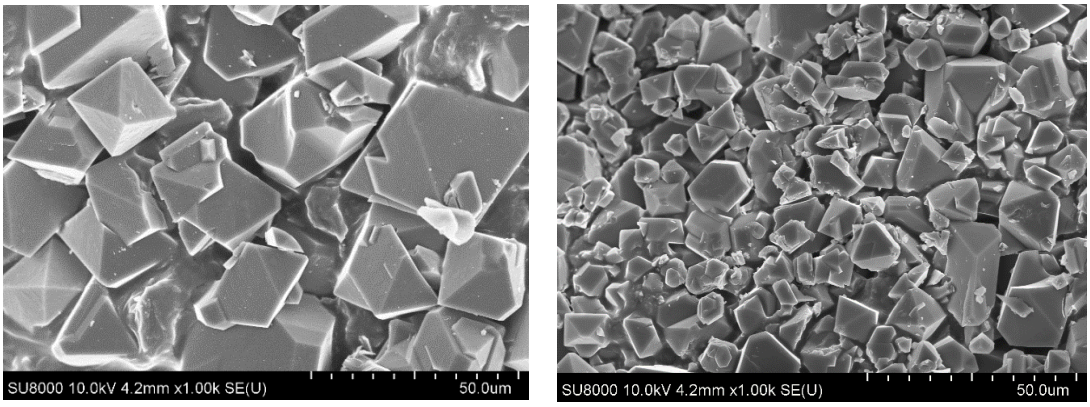

(a) **(b)**

Figure S11. SEM images of the **1mw** (**a**) and **1solv** (**b**) samples [2].

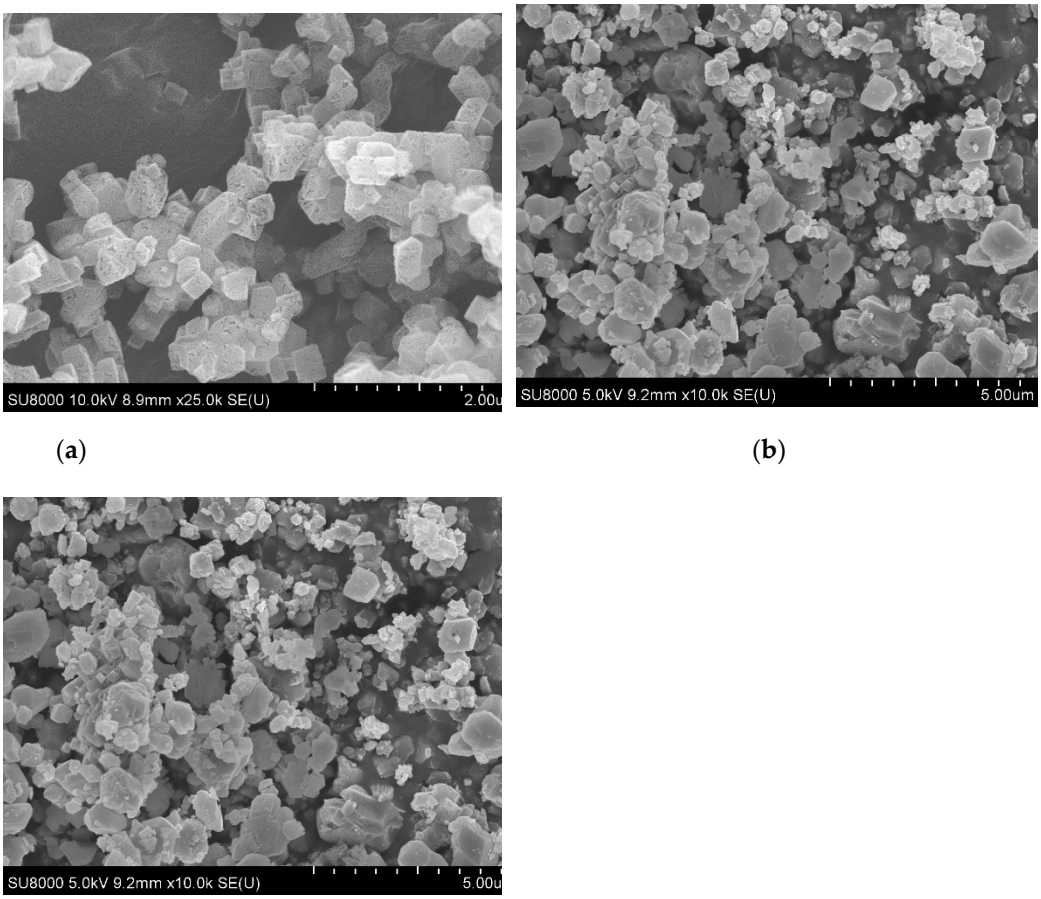

Figure S12. SEM images of the 8solv (**a**), 2solv-after-rinsing (**b**) and 3solv-after-rinsing (**c**) samples.

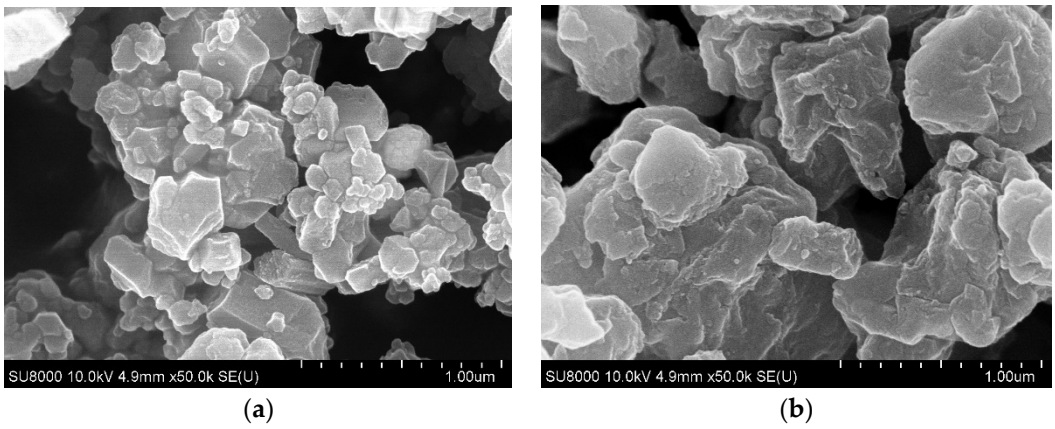

Figure S13. SEM images of the **6mw** (a) and **7mw** (b) samples.

VIII. Thermal stability of the synthesized HKUST-1 materials

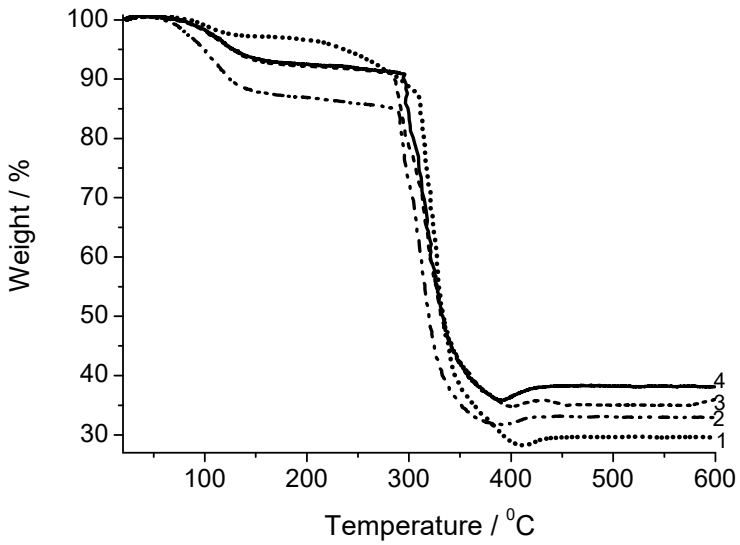

Figure S14. TG Curves of the **1mw** (1), **8solv** (2), **5mw** (3) and **7mw** (4) materials.

IX. DRIFTS study

The Figure S15 shows DRIFT spectra of the **5mw** sample and ionic liquid OMIM OTf in a wide range (a) and 1800-750 cm^{-1} region (b), correspondingly.

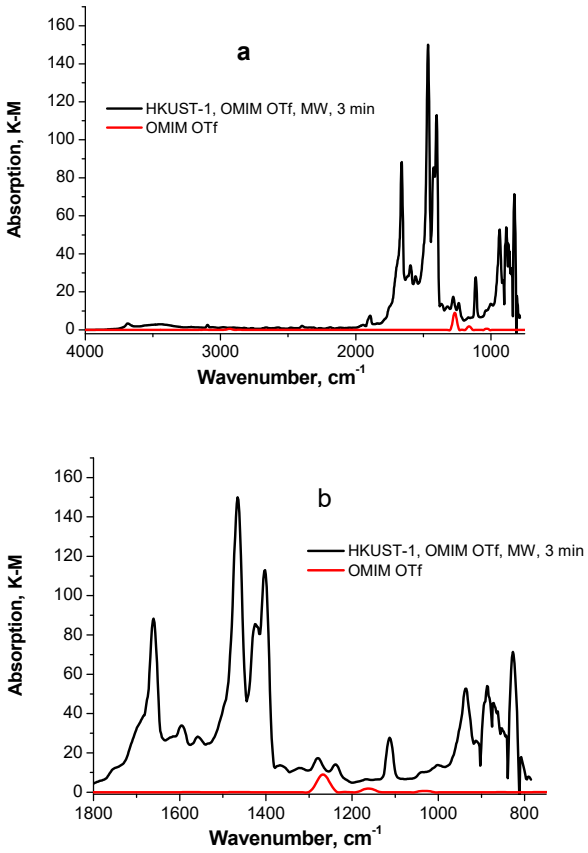

Figure S15. DRIFT spectra of the **5mw** sample and ionic liquid OMIM OTf in a wide range (a) and 1800-750 cm^{-1} region (b), correspondingly.

The Figure S16 shows DRIFT spectra of the **7mw** sample and ionic liquid EMIM Tf_2N in a wide range (a) and 1800-750 cm^{-1} region (b), correspondingly.

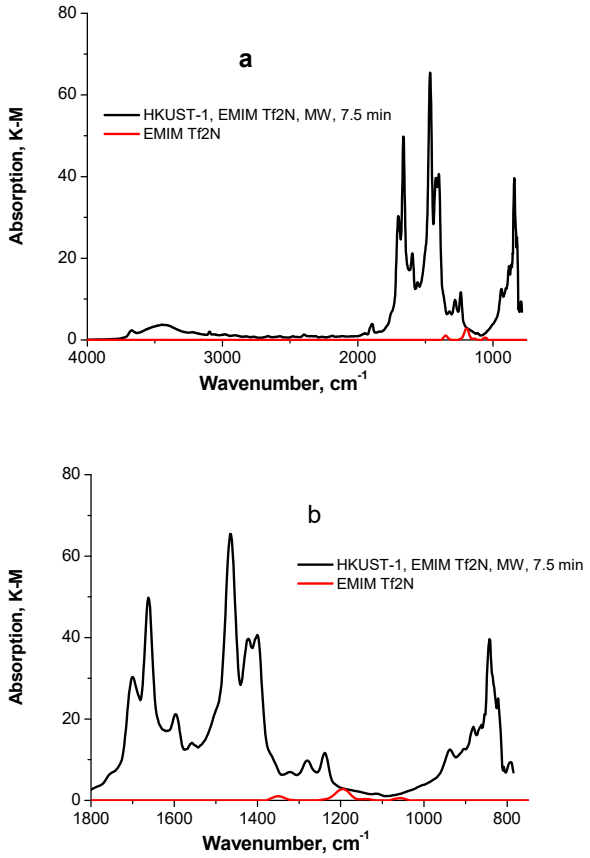

Figure S16. DRIFT spectra of the **7mw** sample and ionic liquid EMIM Tf_2N in a wide range (a) and 1800-750 cm^{-1} region (b), correspondingly.

The Figure S17 shows the comparison of DRIFT spectra recorded for the **5mw**, **7mw** and **8solv** materials.

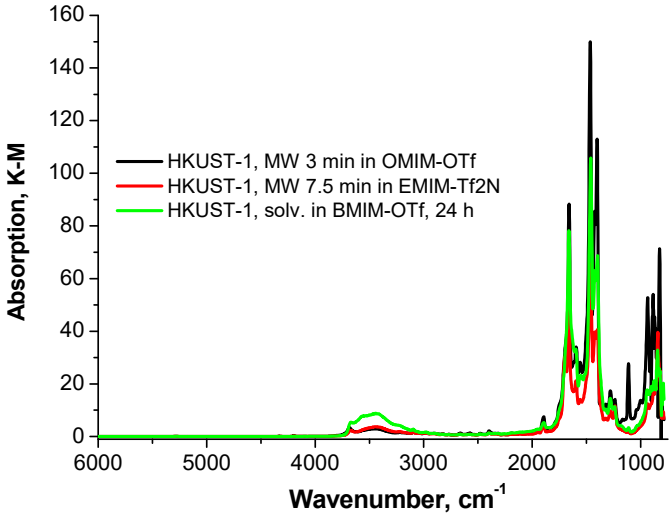

Figure S17. DRIFT spectra of **5mw** (black), **7mw** (red) and **8solv** (green) samples.

Figures S18 and S19 compare the spectra of these samples in two frequency ranges in which absorption bands appear.

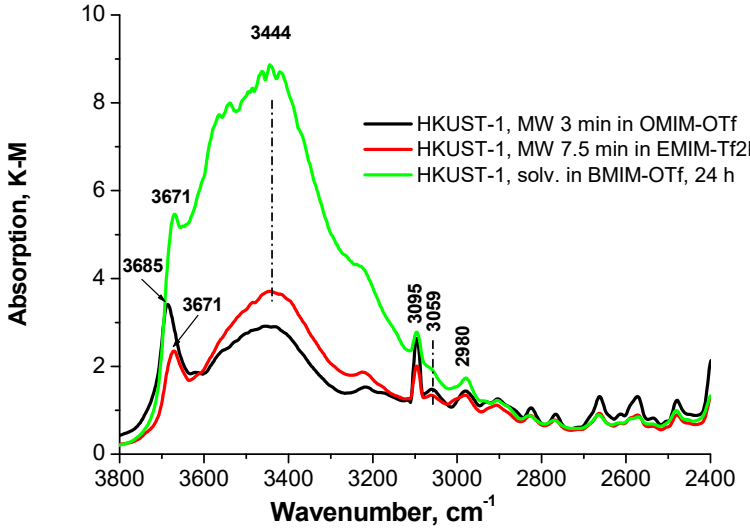

Figure S18. DRIFT spectra of **5mw** (black), **7mw** (red) and **8solv** (green) samples in the frequency range of 3800-2400 cm^{-1}.

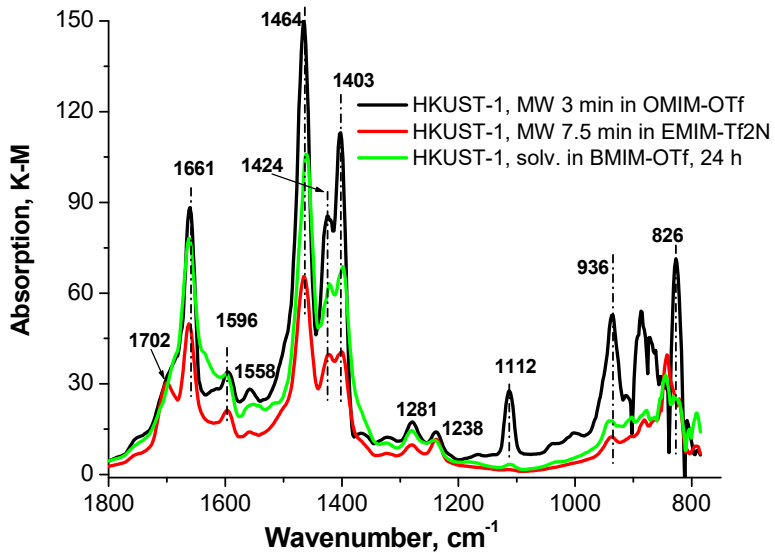

Figure S19. DRIFT spectra of **5mw** (black), **7mw** (red) and **8solv** (green) samples in the frequency range of 1800-750 cm^{-1}.

There are broad intensive bands at 3800-3000 cm^{-1} in the spectra of **5mw**, **7mw** and **8solv** samples (Fig. S18) with maximum at 3444 cm^{-1}. This region corresponds to the stretching vibration of OH groups connected by a weak hydrogen bond. At the same time the absence of the bands in the spectra around 5200 cm^{-1} makes it possible to exclude the presence of adsorbed water.

Moreover, there are sharp bands at 3685 cm^{-1} (**5mw** sample) and 3671 cm^{-1} in both **7mw** and **8solv** samples that show the presence of isolated OH-groups (Fig. S18). There are bands belongs to the C-H bond in aromatic rings in the same region. The bands at 3095-3059 и 2980 $см^{-1}$ (Fig. S18) characterize asymmetrical and symmetrical stretching vibrations in $–CH_3$ и $–CH_2$ fragments.

In spectrum of the **5mw** sample (Fig. S18), the bands at 1661 cm^{-1} are present. DRIFT spectra of all three samples (**5mw**, **7mw** and **8solv**) are similar (Fig. S19). There are bands 1702, 1661, 1596, 1558, 1464, 1424, 1403, 1281, 1238, 1112, 936 and 826 cm^{-1}. These bands characterize the HKUST-1 framework vibrations. In the region between 1700 and 1300 cm^{-1} there are band of the carboxylate ligands. The bands at 1661 и 1596 cm^{-1} and at 1464 and 1403 cm^{-1} characterize asymmetrical and symmetrical stretching vibrations carboxylate groups in carboxylic acids.

X. Adsorption experiments

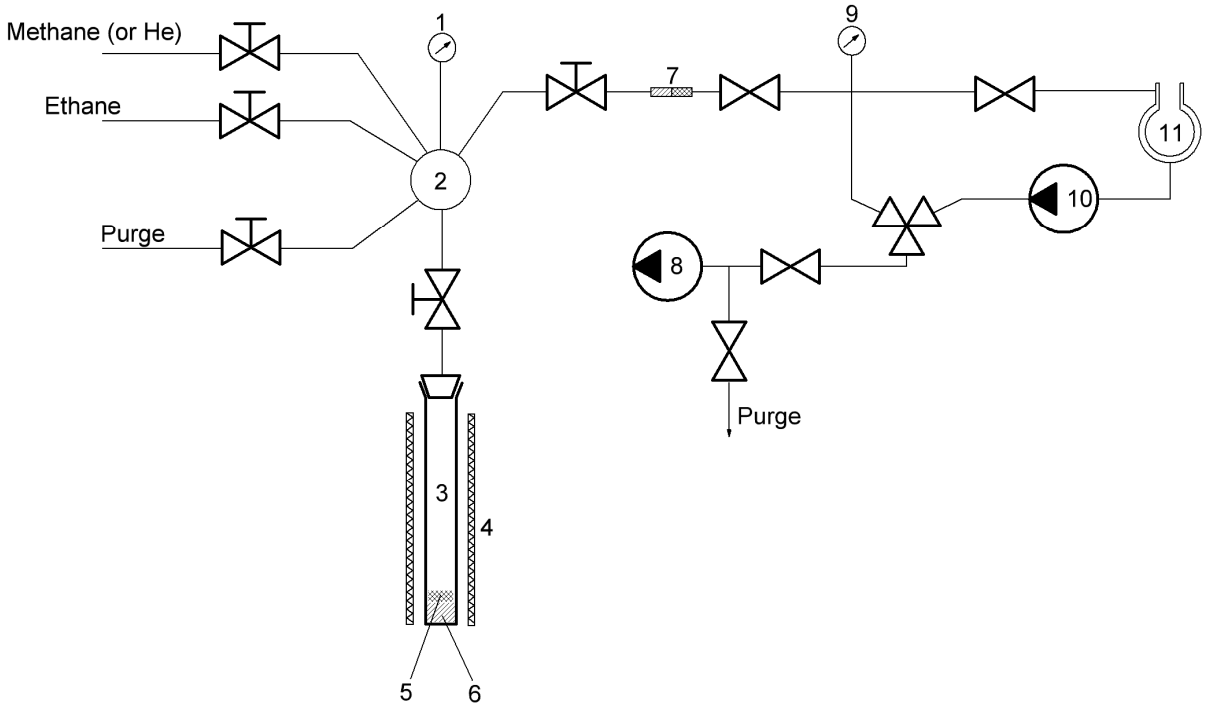

Figure S20. The schematic diagram of the adsorption setup. 1. Manometer. 2. Gas line connector. 3. Adsorption cell. 4. Heater. 5. Glass fabric filter. 6. Sample. 7. Glass-metal connector (Kovar). 8. Rotary pump. 9. Vacuum meter (Pirani gauge). 10. Three-stage oil diffusion pump. 11. Trap with liquid nitrogen (Dewar flask).

Adsorption isotherms were measured at 298 K. The schematic diagram of the adsorption setup is shown in Fig. S9. The high-pressure part of the setup is made from stainless steel, and the vacuum part is made of glass. The system volume of the unit is 20.66 cm^3,

the adsorption cell volume is 9.635 cm^3. The adsorption cell has a gasket-free stainless steel cone-cone seal connector ensuring constancy of the cell volume in each experiment. Before measurements, the samples were evacuated at 140°C at a residual pressure $<3 \cdot 10^{-4}$ Torr. The pressure in the adsorption circuit was measured with a DM5002M digital manometer (Manotom, Russia), 1–40 atm gauge pressure range, 0.1% f.s. precision). The sample volume was determined by helium pycnometry. The adsorption equilibrium was attained in 2-3 h. The total error determined in blank experiments (empty reactor) with the same number of measurement points was less than 0.1 mmol for ethane and 0.05 mmol for methane (at 30 atm).

Empirical equations of state for methane and ethane

The gas densities of methane and ethane were calculated by numerically solving the high precision equation of states (1) taken from [3, 4]. The calculated gas densities at each pressure were used to determine the adsorption values at an equilibrium pressure.

$$\frac{pV}{RT} = 1 + \sum_{i=1} \sum_{j=0} b_{ij} \frac{\left(\frac{\rho}{\rho_{cr.}}\right)^i}{\left(\frac{T}{T_{cr.}}\right)^j} \quad (1)$$

where p – gas pressure (Pa), V – volume (m^3), R – gas constant (J/(kg K)), T – current temperature (K), $T_{cr.}$ – critical temperature (K), $\varrho_{cr.}$ – critical density (kg/m^3), b_{ij} – empirical parameters.

The accuracy of the calculations was thoroughly checked using the density data tables for each gas from the same works [3, 4].

The following parameters were used for each gas:

Ethane [3] – R = 276.507 J/(kg K), $T_{cr.}$ = 305.33 K, $\varrho_{cr.}$ = 204.457 kg/m^3

b[i, j] coefficients for ethane:

b[1,0]=0.6523112;b[1,1]=-1.420959;b[1,2]=-0.8281694;b[1,3]=0.9628378;
b[1,4]=-0.4873274;b[1,5]=-0.1120178;b[1,6]=0.04053669;b[1,7]=0.006643199;
b[2,0]=-0.17173;b[2,1]=1.342033;b[2,2]=-0.5419403;b[2,3]=-0.3585280;
b[2,4]=0.3413308;b[2,5]=-0.1419773;b[2,6]=-0.083274;
b[3,0]=0.1816776;b[3,1]=-1.159004;b[3,2]=0.06856036;
b[3,3]=0.4834712;b[3,4]=0.3294358;b[3,5]=0.2712144;
b[4,0]=0.07302986;b[4,1]=0.6713792;b[4,2]=-0.4315169;
b[4,3]=-0.1305074;b[4,4]=-0.2605725;b[4,5]=-0.01298954;
b[5,0]=-0.03324578;b[5,1]=0.08053416;b[5,2]=0.07465193;
b[5,3]=0.05459819;b[5,4]=-0.03786991;
b[6,0]=-0.1392303;b[6,1]=-0.02013963;b[6,2]=-0.09262326;
b[6,3]=-0.03878733;b[6,4]=0.01381212;
b[7,0]=0.1066015;b[7,1]=-0.02039723;b[7,2]=0.05628173;b[7,3]=0.007784005;
b[8,0]=-0.02233251;b[8,1]=0.02384036;b[8,2]=0.002426002;b[8,3]=-0.00341402;
b[9,0]=-0.01016497;b[9,1]=-0.01018997;b[9,2]=0.002835872;
b[10,0]=0.004957046;b[10,1]=-0.001722518;

Methane [4] – R = 518.271 J/(kg K), $T_{cr.}$ = 190.77 K, $\rho_{cr.}$ = 163.5 kg/m^3

b[i,j] coefficients for methane:

b[1,0]=0.5365574;b[1,1]=-1.671289; b[1,2]=1.704335; b[1,3]=-4.003982;
b[1,4]=3.491415; b[1,5]=-1.332024; b[1,6]=0.05440249; b[1,7]=0.05211075;
b[2,0]=0.07187518; b[2,1]=0.5481658; b[2,2]=-1.932578; b[2,3]=4.295984;
b[2,4]=-3.969273; b[2,5]=1.944849; b[2,6]=-0.5923964;
b[3,0]=0.04802716; b[3,1]=0.1443345; b[3,2]=-1.249822; b[3,3]=1.618220;
b[3,4]=-1.690813; b[3,5]=1.154217; b[3,6]=0.09352795;
b[4,0]=0.02431204; b[4,1]=0.3478417; b[4,2]=0.03587548;
b[4,3]=0.2945131;b[4,4]=0.01565847; b[4,5]=-0.4257759;
b[5,0]=-0.1779964;b[5,1]=-0.02754465; b[5,2]=-0.5843797;
b[5,3]=0.2273617; b[5,4]=-0.07393567; b[5,5]=0.01461452;
b[6,0]=0.1650834; b[6,1]=0.1337959; b[6,2]=0.1158357;
b[6,3]=-0.1025381; b[6,4]=0.07468426; b[7,0]=-0.08863694;
b[7,1]=-0.06837762; b[7,2]= 0.05915308; b[7,3]=0.00298552;
b[8,0]=0.03030236; b[8,1]=-0.001014545; b[8,2]=-0.01847890;
b[8,3]=-0.003250667; b[9,0]=-0.006183691; b[9,1]=0.006643026;
b[9,2]=0.0009014904; b[9,3]=-0.0008454372;
b[10,0]=0.000610039; b[10,1]=-0.001371245; b[10,2]=0.0006833971.

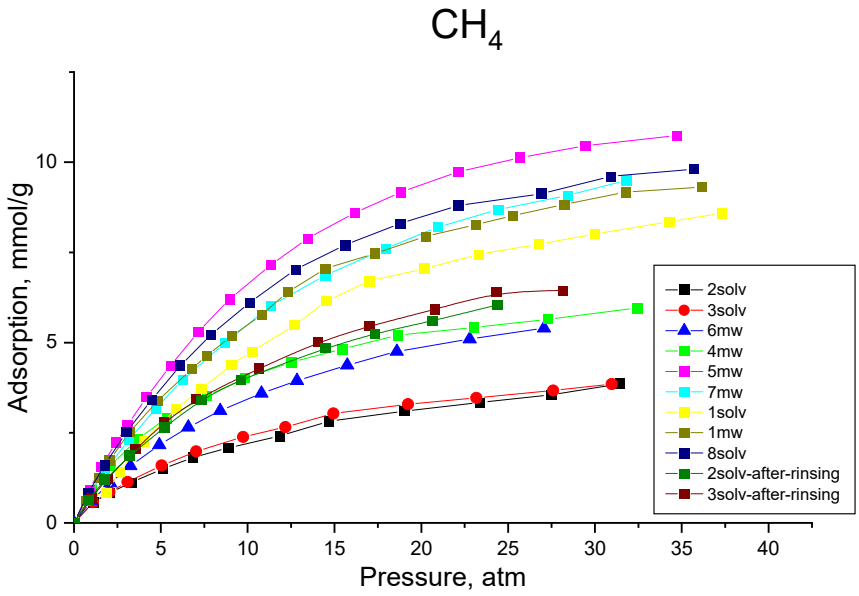

Figure S21. Methane adsorption isotherms for all obtained samples at 298 K.

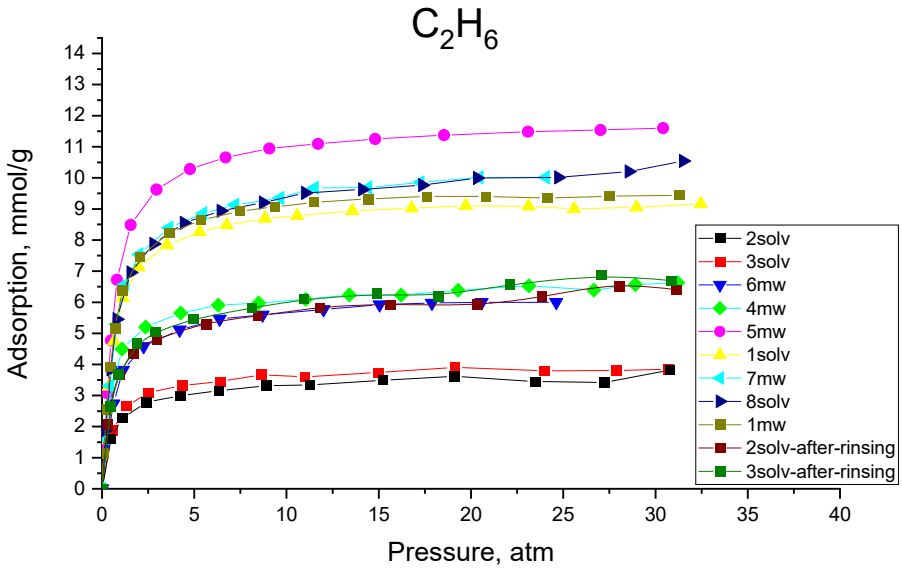

Figure S22. Ethane adsorption isotherms for all obtained samples at 298 K.

References:

1. Pawley, G.S. Unit-cell refinement from powder diffraction scans. *J. Appl. Crystallogr.* ***1981***, *14*, *357–361*, doi:10.1107/S0021889881009618.
2. Isaeva, V. I.; Saifutdinov, B. R.; Chernyshev, V. V.; Vergun, V. V.; Kapustin, G. I.; Kyrnysheva, Yu. P.; Ilyin, M. M.; Kustov, L. M. *Molecules* **2020**, *25*, 2648; doi:10.3390/molecules25112648.
3. Sychev, V. V.; Wasserman, A. A.; Zagoruchenko, V. A.; Kozlov, A. D.; Spiridonov, G. A.; Tsymarnyi, V. A. *Thermodynamic properties of ethane*; Izdatel'stvo Standartov: Moscow, Russia, 1982; 305p. (In Russian).
4. Sychev, V. V.; Wasserman, A. A.; Zagoruchenko, V. A.; Kozlov, A. D.; Spiridonov, G. A.; Tsymarnyi, V. A. *Thermodynamic properties of methane*; Izdatel'stvo Standartov: Moscow, Russia, 1979; 351p. (In Russian).